

F-bar aided edge-based smoothed finite element methods with 4-node tetrahedral elements for static large deformation hyperelastic and elastoplastic problems

Yuki Onishi^{1,a)}, Ryoya Iida¹ and Kenji Amaya¹

¹ Department of Systems and Control Engineering, Tokyo Institute of Technology, Japan

^{a)}Corresponding and Presenting author: onishi.y.ad@m.titech.ac.jp

ABSTRACT

A new type of smoothed finite element method, F-barES-FEM-T4, is demonstrated in static large deformation hyperelastic and elastoplastic cases. F-barES-FEM-T4 combines NS-FEM-T4 and ES-FEM-T4 with the aid of F-bar method in order to resolve all the major issues of Selective ES/NS-FEM-T4: limitation of material models, pressure oscillation, and corner locking. As well as other S-FEMs, F-barES-FEM-T4 inherits displacement-based formulation and thus has no increase in DOF. Moreover, the cyclic smoothing procedure introduced in F-barES-FEM-T4 is effective to adjust the smoothing level so that pressure oscillation is suppressed reasonably. A few examples of analyses for rubber-like hyperelastic and elastoplastic materials proof the excellent performance of F-barES-FEM-T4 in contrast to the conventional hybrid elements.

Keywords: Smoothed finite element method, F-bar method, Large deformation, Cyclic smoothing, Pressure oscillation, Locking-free.

Introduction

In the practical use of the finite element method (FEM) for complex shapes, analyses with tetrahedral meshes are indispensable. However, the standard 4-node linear (constant strain) tetrahedral (T4) element has many accuracy issues such as shear locking. Especially when the incompressibility arises in rubber-like or plastic materials, it also suffers from volumetric locking and pressure oscillation issues. Due to the poor performance of the standard T4 element, there have been many researches on the advanced FE formulations of tetrahedral elements.

The hybrid 10-node quadratic (2nd-order) tetrahedral (T10) elements [1] generally represent good results; however, they have accuracy and convergence problems in severe large deformation analysis or contact analysis because of the presence of intermediate nodes. The hybrid T4 element [1] is also used late years but has accuracy issues [5, 6] and brings significant increase in the degree of freedom (DOF) as well. An alternative approach to this problem is the smoothed finite elements methods (S-FEMs) [3]. Selective ES/NS-FEM-T4 [3, 4] would be one of the current best S-FEM-T4 formulations; yet, it still has three major issues: limitation of material models, pressure oscillation, and corner locking [5]. Recently, we proposed a new type of S-FEM-T4 formulation called F-bar aided edge-based smoothed finite element method (F-barES-FEM-T4) [6]. As the adoption of the F-bar method [2] to combine NS-FEM-T4 and ES-FEM-T4 [3], F-barES-FEM-T4 is able to resolve all the major issues of Selective ES/NS-FEM-T4.

In this study, the effectiveness of F-barES-FEM-T4 in static large deformation analyses is demonstrated not only in rubber-like hyperelastic cases but also in elastoplastic cases. Plastic deformation in progress generally decreases the shear modulus drastically and thus presents near incompressibility, thereby inducing volumetric locking and pressure oscillation frequently. A few examples of analyses show that F-barES-FEM-T4 is locking-free and pressure oscillation-free in elastoplastic analyses as well as in nearly incompressible hyperelastic analyses.

Methods

The presenting method, F-barES-FEM-T4, takes advantages of ES-FEM-T4 and NS-FEM-T4 by combining them with F-bar method [2]. The conceptual illustration of F-barES-FEM-T4 is shown in Fig. 1. In F-barES-FEM-T4, the isovolumetric part of the deformation gradient (\mathbf{F}^{iso}) is evaluated by using ES-FEM-T4, whereas the volumetric part (\mathbf{F}^{vol}) is evaluated

by using NS-FEM-T4 multiply. Combining \mathbf{F}^{iso} and \mathbf{F}^{vol} with F-bar method, the final deformation gradient \mathbf{F} is given at edges in the same manner as ES-FEM-T4.

A brief explanation of F-barES-FEM-T4 is described later in this section. See reference [6] for the detail.

Calculation of $^{\text{Edge}}\widetilde{\mathbf{F}}^{\text{iso}}$

The isovolumetric part of the deformation gradient at each edge, $^{\text{Edge}}\widetilde{\mathbf{F}}^{\text{iso}}$, is given in the same manner as ES-FEM-T4.

$$^{\text{Edge}}\widetilde{\mathbf{F}}^{\text{iso}} = \left(\frac{1}{^{\text{Edge}}\widetilde{J}} \right)^{1/3} ^{\text{Edge}}\widetilde{\mathbf{F}}; \quad (1)$$

$$^{\text{Edge}}\widetilde{\mathbf{F}} = \frac{1}{^{\text{Edge}}V^{\text{ini}}} \sum_{e \in ^{\text{Edge}}\widetilde{\mathbb{E}}} ^{\text{Elem}}\mathbf{F} ^{\text{Elem}}V^{\text{ini}} / 6, \quad (2)$$

$$^{\text{Edge}}\widetilde{J} = \det(^{\text{Edge}}\widetilde{\mathbf{F}}), \quad (3)$$

where $^{\text{Edge}}\widetilde{\mathbb{E}}$ is the set of elements attached to edge h , $^{\text{Edge}}V^{\text{ini}}$ and $^{\text{Elem}}V^{\text{ini}}$ are the initial corresponding volume of edge h and element e , respectively.

Calculation of $^{\text{Edge}}\overline{\mathbf{F}}^{\text{vol}}$

On the other hand, the volumetric part of the deformation gradient at each edge, $^{\text{Edge}}\overline{\mathbf{F}}^{\text{vol}}$, is given by the cyclic smoothing procedure as follows.

- i. Calculate $^{\text{Elem}}\mathbf{F}$ and $^{\text{Elem}}J$ at each element in the same manner as the standard FEM-T4:

$$^{\text{Elem}}F_{ij} = ^{\text{Elem}}N_{P,j}^{\text{ini}} x_{P,i}, \quad (4)$$

$$^{\text{Elem}}J = \det(^{\text{Elem}}\mathbf{F}), \quad (5)$$

where $^{\text{Elem}}N_{P,j}^{\text{ini}}$ is the spatial derivative of the shape function $^{\text{Elem}}N_P^{\text{ini}}$ in the x_j direction and $x_{P,i}$ is the coordinate of node P in the x_i direction.

- ii. Calculate the smoothed J at each node, $^{\text{Node}}\widetilde{J}$, in the same manner as NS-FEM-T4:

$$^{\text{Node}}\widetilde{J} = \frac{1}{^{\text{Node}}V^{\text{ini}}} \sum_{e \in ^{\text{Node}}\widetilde{\mathbb{E}}} ^{\text{Elem}}J ^{\text{Elem}}V^{\text{ini}} / 4, \quad (6)$$

where $^{\text{Node}}\widetilde{\mathbb{E}}$ is the set of elements attached to node n , $^{\text{Elem}}V^{\text{ini}}$ is the initial volume of element e , and $^{\text{Node}}V^{\text{ini}}$ is the initial corresponding volume of node n given by $\sum_{e \in ^{\text{Node}}\widetilde{\mathbb{E}}} ^{\text{Elem}}V^{\text{ini}} / 4$.

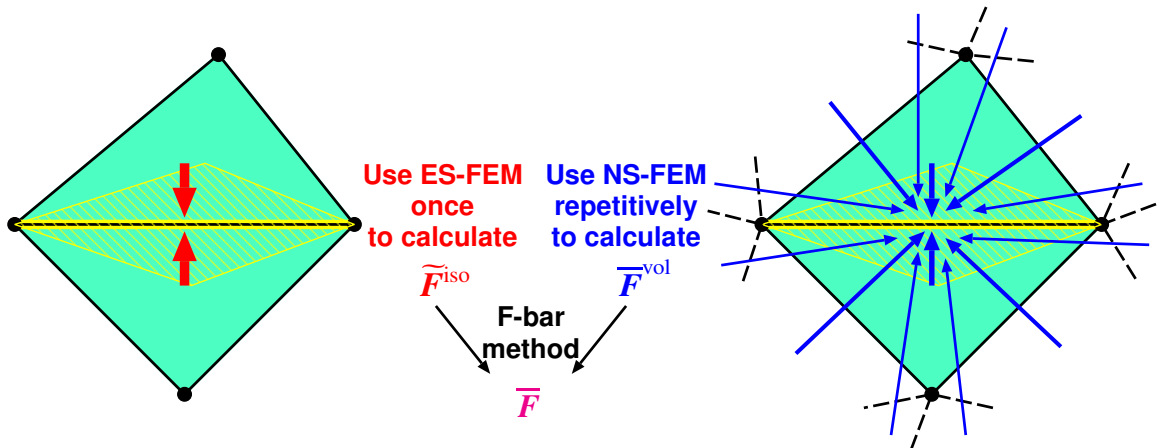


Figure 1. Conceptual illustration of F-barES-FEM.

iii. Calculate the smoothed J at each element, ${}^{\text{Elem}}\tilde{J}$, as follows:

$${}^{\text{Elem}}\tilde{J}_e = \frac{1}{4} \sum_{n \in \text{Elem}_e^{\mathbb{N}}} \text{Node}_n \tilde{J}, \quad (7)$$

where $\text{Elem}_e^{\mathbb{N}}$ is the set of four nodes comprising element e .

iv. Repeat ii. and iii. c times and obtain the multiply smoothed J at each element, ${}^{\text{Elem}}\bar{J}$. Note that ${}^{\text{Elem}}J$ is regarded as ${}^{\text{Elem}}\tilde{J}$ in the second or later evaluation of Eq. (6). Also, ${}^{\text{Elem}}\tilde{J}$ is regarded as ${}^{\text{Elem}}\bar{J}$ in the last evaluation of Eq. (7).

v. Calculate the multiply smoothed J at each edge, ${}^{\text{Edge}}\bar{J}$, in a similar fashion as ES-FEM-T4:

$${}^{\text{Edge}}\bar{J}_h = \frac{1}{{}^{\text{Edge}}V_h^{\text{ini}}} \sum_{e \in \text{Edge}_h^{\mathbb{E}}} {}^{\text{Elem}}\bar{J}_e {}^{\text{Elem}}V_e^{\text{ini}} / 6, \quad (8)$$

where $\text{Edge}_h^{\mathbb{E}}$ is the set of elements attached to edge h and ${}^{\text{Edge}}V_h^{\text{ini}}$ is the initial corresponding volume of edge h given by $\sum_{e \in \text{Edge}_h^{\mathbb{E}}} {}^{\text{Elem}}V_e^{\text{ini}} / 6$.

vi. Calculate the multiply smoothed \mathbf{F}^{vol} at each edge, ${}^{\text{Edge}}\bar{\mathbf{F}}^{\text{vol}}$:

$${}^{\text{Edge}}\bar{\mathbf{F}}^{\text{vol}}_h = {}^{\text{Edge}}\bar{J}_h^{1/3} \mathbf{I}. \quad (9)$$

where \mathbf{I} is the unit tensor.

Note that Eq. (6), (7) and (8) satisfy the partition of unity condition and thus the near incompressibility of rubber-like materials is satisfied at the multi-smoothing domain of each edge.

The number of cyclic smoothing, c , is the tuning parameter of F-barES-FEM-T4. F-barES-FEM-T4 with c -time cyclic smoothing is referred to as ‘‘F-barES-FEM-T4(c)’’ hereafter in this paper.

Calculation of ${}^{\text{Edge}}\bar{\mathbf{F}}$

The final deformation gradient at each edge, ${}^{\text{Edge}}\bar{\mathbf{F}}$, is obtained by combining ${}^{\text{Edge}}\tilde{\mathbf{F}}^{\text{iso}}$ of Eq. (1) and ${}^{\text{Edge}}\bar{\mathbf{F}}^{\text{vol}}$ of Eq. (9) with F-bar method.

$${}^{\text{Edge}}\bar{\mathbf{F}}_h = {}^{\text{Edge}}\bar{\mathbf{F}}^{\text{vol}}_h \cdot {}^{\text{Edge}}\tilde{\mathbf{F}}^{\text{iso}}_h. \quad (10)$$

Calculation of ${}^{\text{Edge}}\mathbf{T}$

The Cauchy stress at each edge, ${}^{\text{Edge}}\mathbf{T}$, is then derived in the standard way with ${}^{\text{Edge}}\bar{\mathbf{F}}$. In case of history-dependent materials such as elastoplastic materials, ${}^{\text{Edge}}\mathbf{T}$ is derived with the history of ${}^{\text{Edge}}\bar{\mathbf{F}}$.

Calculation of ${}^{\text{Edge}}f^{\text{int}}$

The contribution of each edge to the nodal internal force, ${}^{\text{Edge}}f^{\text{int}}$, is calculated in manner of the F-bar method as

$${}^{\text{Edge}}f_{P;p}^{\text{int}} = \frac{\partial {}^{\text{Edge}}\tilde{D}_{ij}}{\partial u_{P;p}} {}^{\text{Edge}}T_{pl} {}^{\text{Edge}}V_h. \quad (11)$$

Note that the stretching tensor in this equation, ${}^{\text{Edge}}\tilde{D}$, is not the deformation rate of ${}^{\text{Edge}}\bar{\mathbf{F}}$ in Eq. (10) but that of ${}^{\text{Edge}}\tilde{\mathbf{F}}$ in Eq. (2).

Results

Barreling of Hyperelastic Cylinder

A hyperelastic large deformation analysis of a 1/8 cylinder with enforced displacements is performed. Figure 2 illustrates the outline of the analysis. Barreling deformation grows as the enforced displacement progresses, and then the lateral

surface is squeezed out. The material constitutive model of the cylinder is the neo-Hookean hyperelastic model, $\mathbf{T} = 2C_{10} \frac{\text{Dev}(\bar{\mathbf{B}})}{J} + \frac{2}{D_1}(J-1)\mathbf{I}$, where $C_{10} = 4 \times 10^7$ Pa and $D_1 = 5 \times 10^{-11}$ Pa⁻¹ and thus the initial Poisson's ratio is 0.499. The mesh seed size is 0.05(= 1/20) m constant for 1st-order elements and is 0.1(= 1/10) m constant for 2nd-order elements.

Firstly, results of 4-node hybrid tetrahedral element of ABAQUS/Standard (ABAQUS C3D4H), 10-node quadratic modified hybrid tetrahedral element (ABAQUS C3D10MH), and 8-node hybrid hexahedral element (ABAQUS C3D8H) are shown in Figs. 3–5. ABAQUS C3D4H is free from shear and volumetric locking; however, it has two major issues: pressure oscillation and corner locking [5]. The corner locking is a type of locking that brings a strangely hard deformation around corners in large deformation cases. ABAQUS C3D10MH is free from shear, volumetric, and corner locking; how-

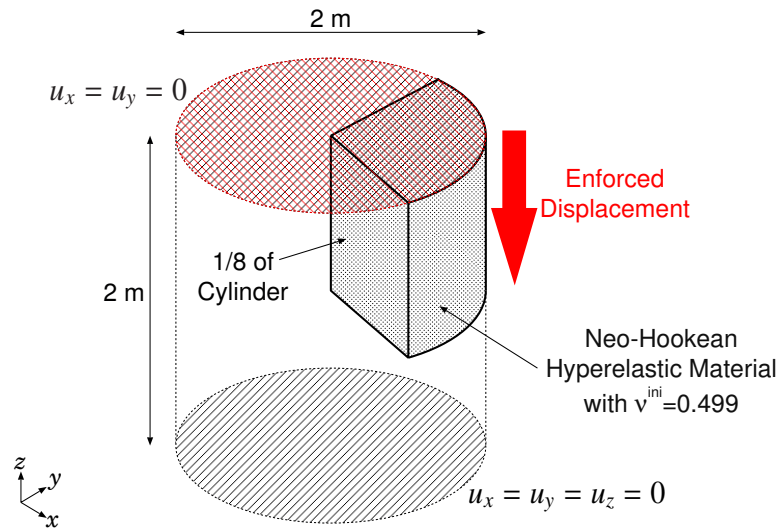


Figure 2. Outline of the hyperelastic barreling analysis.

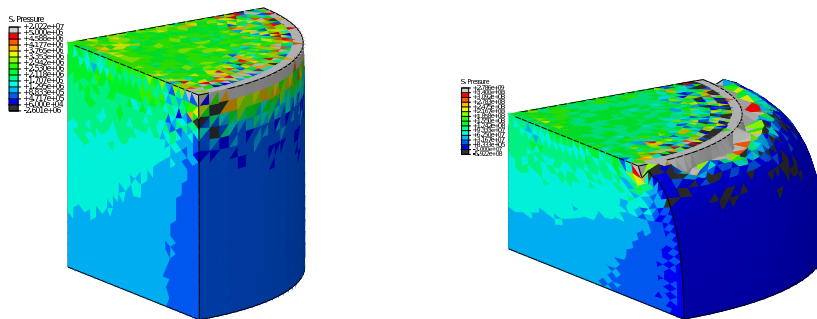


Figure 3. Pressure distributions of ABAQUS C3D4H results. Left: $u_z = 0.01$ m. Right: $u_z = 0.40$ m.

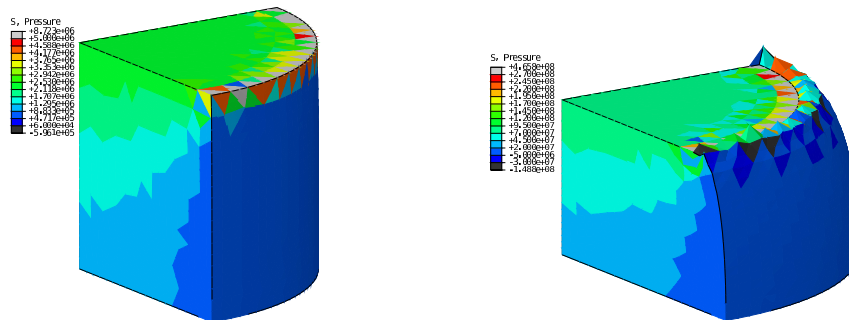


Figure 4. Pressure distributions of ABAQUS C3D10MH results. Left: $u_z = 0.01$ m. Right: $u_z = 0.32$ m.

ever, it suffers from convergence failure in a relatively earlier stage. Moreover, the presence of intermediate nodes causes accuracy loss of interpolation in large deformation cases. ABAQUS C3D8H is also free from shear, volumetric, and corner locking; however, it suffers from pressure oscillation.

Secondly, results of Selective ES/NS-FEM-T4, F-barES-FEM-T4(1), (2), (3) and (4) are shown in Figs. 6–10. Selective ES/NS-FEM-T4 and all F-barES-FEM-T4s are free from shear and volumetric locking and have no convergence problem. Selective ES/NS-FEM-T4 and F-barES-FEM-T4(1) have pressure oscillation and corner locking issues, whereas F-barES-FEM-T4(2) or later suppresses these issues. It should be noted that F-barES-FEM-T4(2) or later are not much different each other and thus c is not much sensitive to the result. Therefore, F-barES-FEM-T4 with a sufficient cycles of smoothing c resolves all the accuracy issues of conventional methods.

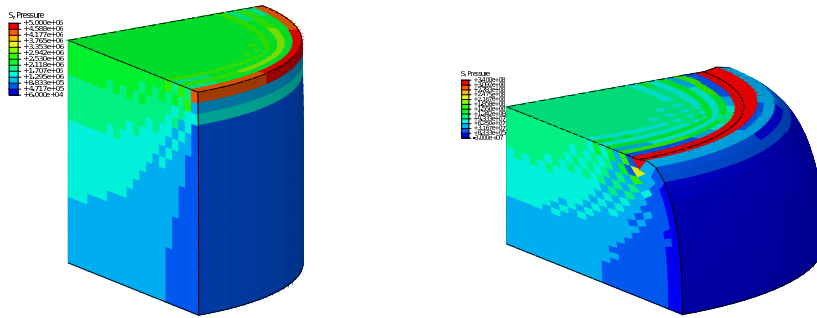


Figure 5. Pressure distributions of ABAQUS C3D8H results. Left: $u_z = 0.01$ m. Right: $u_z = 0.40$ m.

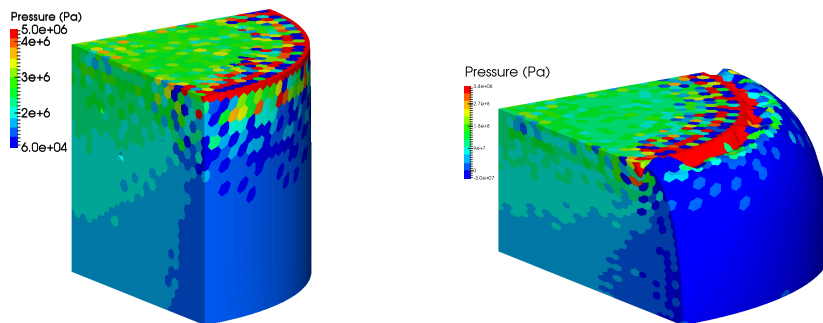


Figure 6. Pressure distributions of Selective ES/NS-FEM-T4 results. Left: $u_z = 0.01$ m. Right: $u_z = 0.40$ m.

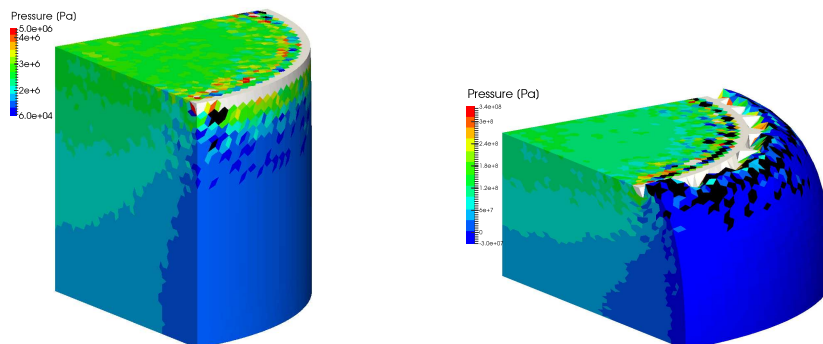


Figure 7. Pressure distributions of F-barES-FEM-T4(1) results. Left: $u_z = 0.01$ m. Right: $u_z = 0.40$ m.

Shear-Tensioning of Elastoplastic Bar

An elastoplastic large deformation analysis of a bar with enforced displacements is performed. Figure 11 illustrates the outline of the analysis. Shear deformation dominates at the middle part of the bar in the early stage of the analysis, whereas stretch deformation dominates in the later stage. The material constitutive model of the bar is the elastoplastic model with Hencky's strain measure, von Mises yield criterion, and the isotropic hardening flow rule. The material properties are 1 GPa Young's modulus, 0.3 Poisson's ratio, 1 MPa yield stress, and 0.1 GPa constant work hardening rate. Hence, the Poisson's ratio under large plastic deformation in progress is greater than 0.48. The mesh seed size is 0.2(= 1/5) m constant.

Results of ABAQUS C3D4H and F-barES-FEM-T4(2) are shown in Fig. 12 and 13. Figure 12 compares the deformations and distributions of the equivalent plastic strain, while Figure 13 compares those of the pressure. The results of ABAQUS

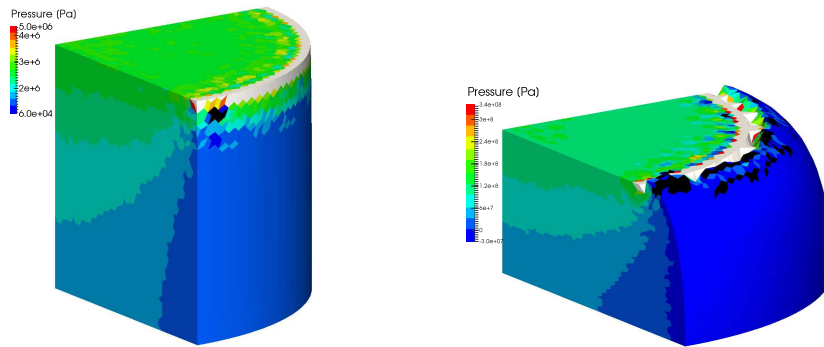


Figure 8. Pressure distributions of F-barES-FEM-T4(2) results. Left: $u_z = 0.01$ m. Right: $u_z = 0.40$ m.

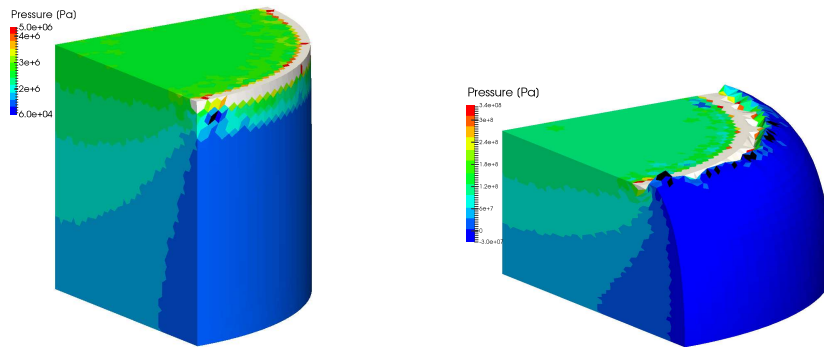


Figure 9. Pressure distributions of F-barES-FEM-T4(3) results. Left: $u_z = 0.01$ m. Right: $u_z = 0.40$ m.

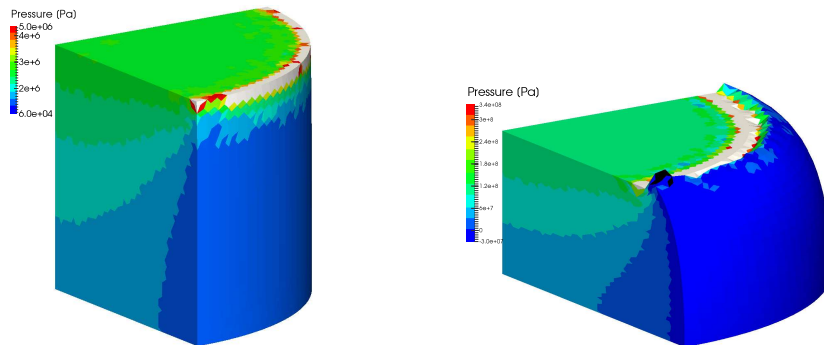


Figure 10. Pressure distributions of F-barES-FEM-T4(4) results. Left: $u_z = 0.01$ m. Right: $u_z = 0.40$ m.

C3D4H represent strange spatial oscillation on both the equivalent plastic strain and pressure distributions. On the other hand, the results of F-barES-FEM-T4(2) are smooth in the both distributions and thus seem valid. F-barES-FEM-T4 is considered effective not only for rubber-like materials but also for elastoplastic materials.

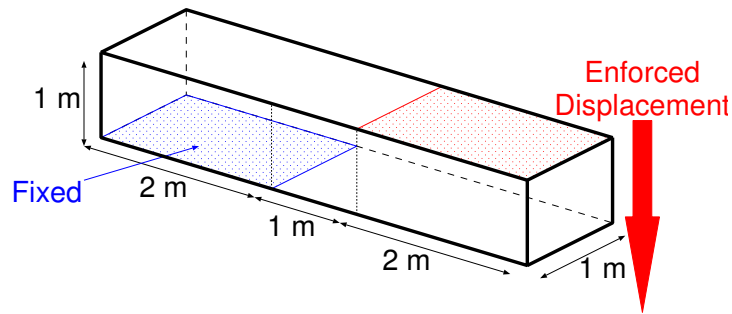


Figure 11. Outline of the elastoplastic shear-tensioning analysis.

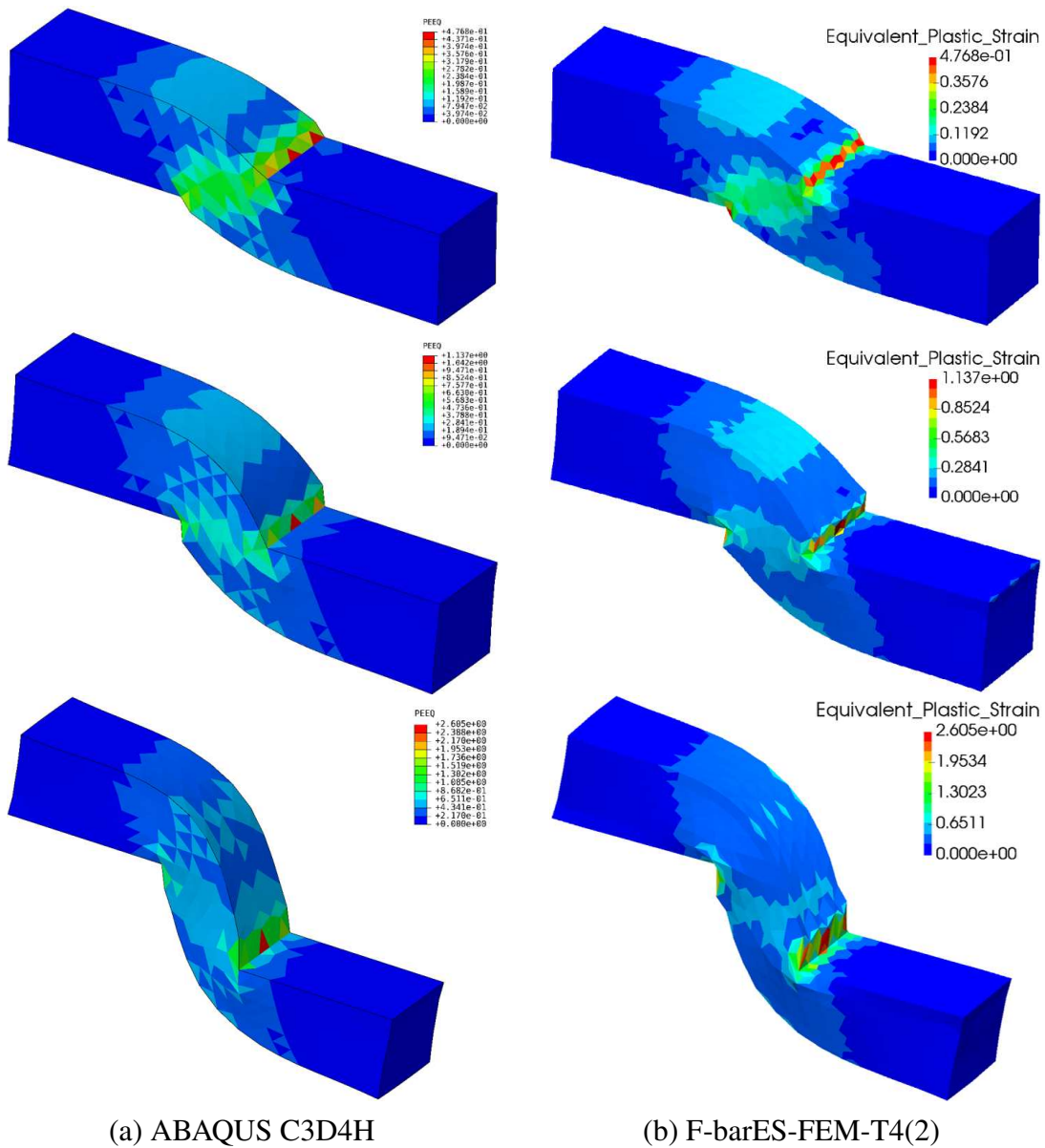


Figure 12. Comparison of equivalent plastic strain distributions on the elastoplastic shear-tensioning analysis.

Conclusion

A new type of smoothed finite element method, F-barES-FEM-T4, is demonstrated in static large deformation hyperelastic and elastoplastic problems. The characteristics of F-barES-FEM-T4 are summarized as follows.

- No increase in DOF.
- No limitation of material models.
- No convergence problem in large deformation.
- Free from shear, volumetric, and corner locking.
- Suppress pressure oscillation in rubber-like/elastoplastic materials.
- Adjustable smoothing level with the number of cyclic smoothings (c).

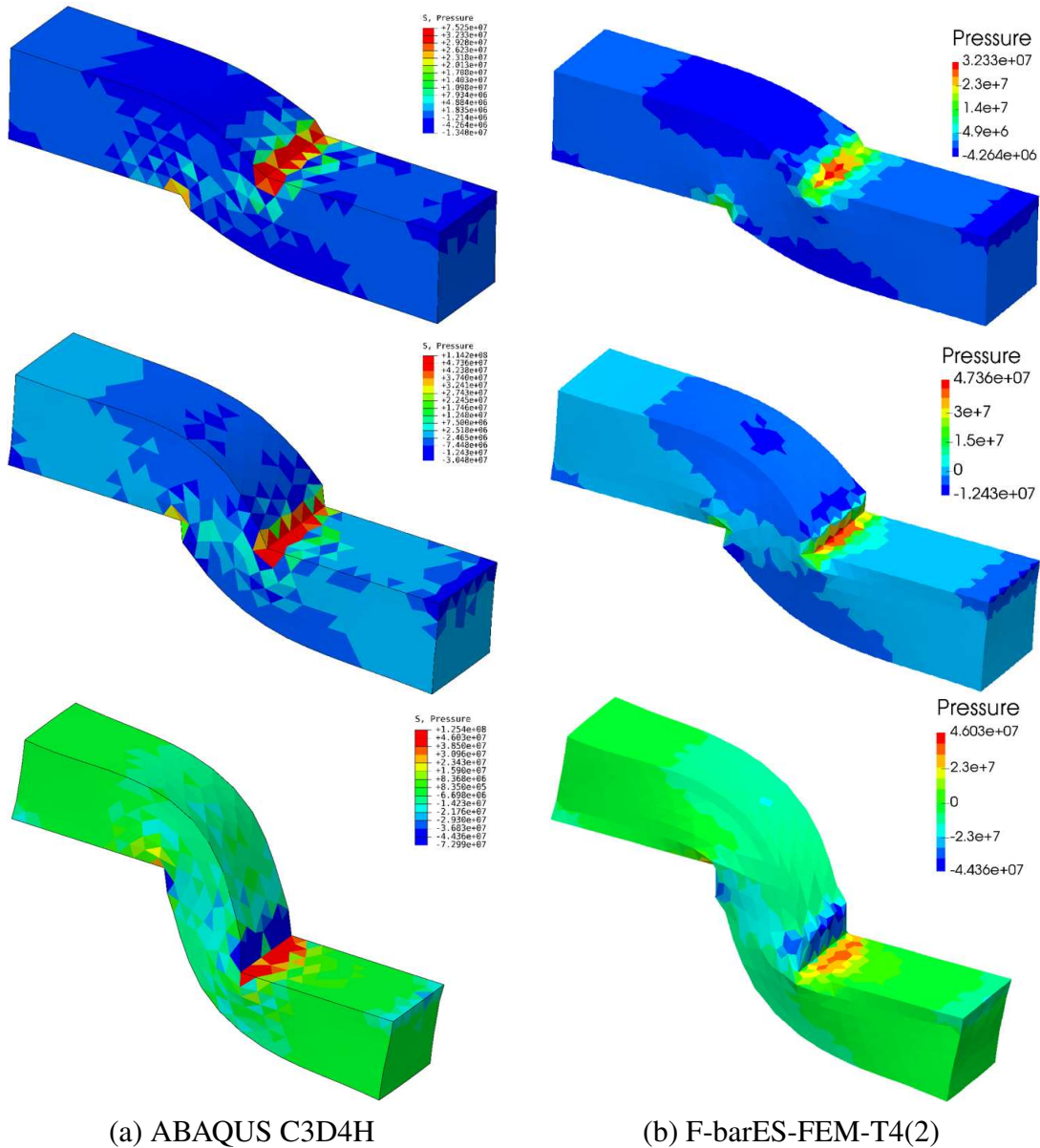


Figure 13. Comparison of pressure distributions on the elastoplastic shear-tensioning analysis.

References

- [1] Dassault Systèmes Simulia Corp. (2013). *ABAQUS 6.13 Theory Guide*. Dassault Systèmes Simulia Corp., Providence, RI, USA.
- [2] de Souza Neto, E., Peric, D., Dutko, M., and Owen, D. (1996). Design of simple low order finite elements for large strain analysis of nearly incompressible solids. *International Journal of Solids and Structures*, 33(20-22):3277–3296.
- [3] Liu, G. R. and Nguyen-Thoi, T. (2010). *Smoothed Finite Element Methods*. CRC Press, Boca Raton, FL, USA.
- [4] Onishi, Y. and Amaya, K. (2014). A locking-free selective smoothed finite element method using tetrahedral and triangular elements with adaptive mesh rezoning for large deformation problems. *International Journal for Numerical Methods in Engineering*, 99(5):354–371.
- [5] Onishi, Y. and Amaya, K. (2015). Performance evaluation of the selective smoothed finite element methods using tetrahedral elements with deviatoric/hydrostatic split in large deformation analysis. *Theoretical and Applied Mechanics Japan*, 63:55–65.
- [6] Onishi, Y., Iida, R., and Amaya, K. (under review). F-bar aided edge-based smoothed finite element method using tetrahedral elements for finite deformation analysis of nearly incompressible solids. *International Journal for Numerical Methods in Engineering*.